

ReRoGCRL: Representation-based Robustness in Goal-Conditioned Reinforcement Learning

Xiangyu Yin¹, Sihao Wu^{*1}, Jiaxu Liu¹, Meng Fang¹, Xingyu Zhao²,
Xiaowei Huang¹, Wenjie Ruan^{1†}

¹ Department of Computer Science, University of Liverpool, Liverpool, L69 3BX, UK

² WMG, University of Warwick, Coventry, CV4 7AL, UK

{X.Yin22;sihao.wu;xiaowei.huang}@liverpool.ac.uk, xingyu.zhao@warwick.ac.uk, w.ruan@trustai.uk

Abstract

While Goal-Conditioned Reinforcement Learning (GCRL) has gained attention, its algorithmic robustness, particularly against adversarial perturbations, remains unexplored. Unfortunately, the attacks and robust representation training methods specifically designed for traditional RL are not so effective when applied to GCRL. To address this challenge, we propose the *Semi-Contrastive Representation* attack, a novel approach inspired by the adversarial contrastive attack. Unlike existing attacks in RL, it only necessitates information from the policy function and can be seamlessly implemented during deployment. Furthermore, to mitigate the vulnerability of existing GCRL algorithms, we introduce *Adversarial Representation Tactics*. This strategy combines *Semi-Contrastive Adversarial Augmentation* with *Sensitivity-Aware Regularizer*. It improves the adversarial robustness of the underlying agent against various types of perturbations. Extensive experiments validate the superior performance of our attack and defence mechanism across multiple state-of-the-art GCRL algorithms. Our tool **ReRoGCRL** is available at <https://github.com/TrustAI/ReRoGCRL>.

Introduction

Goal-Conditioned Reinforcement Learning (GCRL) trains an agent to learn skills in the form of reaching distinct goals. Unlike conventional RL, GCRL necessitates the agent to make decisions aligned with goals. This attribute allows agents to learn and accomplish a variety of tasks with shared knowledge, better generalization, and improved exploration capabilities. Furthermore, it is binary-rewarded, which is easier to implement compared to hand-crafted complex reward functions. Recently, there has been a significant surge in research related to GCRL. Exemplary works include methods based on various techniques, such as hindsight experience replay (Andrychowicz et al. 2018; Fang et al. 2018, 2019), imitation learning (Ghosh et al. 2020; Yang et al. 2021b), or offline learning (Chebotar et al. 2021; Ma et al. 2022; Mezghani et al. 2023).

Generally, the aforementioned studies tend to assume that the sensing and perception systems of agents are devoid of

uncertainties. However, this presumption is hardly applicable in real-world scenarios because there are differences between simulated and real-world environments, such as measurement errors, motor noise, etc. The observations made by robots encompass unavoidable disturbances that originate from unforeseeable stochastic noises or errors in sensing. For example, due to the existence of adversarial attacks in RL agents (Huang et al. 2017; Weng et al. 2019; Bai, Guan, and Wang 2019; Kamalaruban et al. 2020), even minor perturbations can lead to unstable outcomes in the safety-critical GCRL control strategy.

Recently numerous robust techniques have been implemented in traditional RL, which can be broadly classified into two categories: (1) Adversarial Training (AT), and (2) Robust Representation Training. Particularly, AT in RL trains the agents with adversarial states or actions (Pinto et al. 2017; Kos and Song 2017; Zhang et al. 2020b), and then enhance their adversarial robustness. However, AT-trained RL agents cannot be utilized across downstream tasks, which limits their transferability. Compared to AT, robust representation training can deliver *low-dimentional*, *collapse-resistant*, and *perturbation-robust* representations of observations (Gelada et al. 2019; Zhang et al. 2020a; Zang, Li, and Wang 2022), which is the focus of recent studies. Specifically, it learns representations that capture only task-relevant information based on the bisimulation metric of states (Ferns, Panangaden, and Precup 2011). Technically, they minimize the *behavioral difference* between representations of similar observation pairs in the latent space.

Although there are already many articles enhancing the robustness of RL, few works (He and Lv 2023) consider the robustness of GCRL against adversarial perturbations. Different from the vanilla one, GCRL employs reward functions characterized by sequences of unshaped binary signals. For example, (Andrychowicz et al. 2018) allocates the reward by determining whether the distance between the achieved goal \hat{g} and the desired goal g is less than a threshold ϵ : $\mathbb{1}(\|\hat{g} - g\| \leq \epsilon)$. This makes the reward sequences in GCRL notably sparser than those in traditional RL. However, the sparsity of rewards in GCRL leads to inaccurate estimations of Q-values and actions, and challenges the direct application of traditional RL attacks, especially those dependent on pseudo labels, such as Q-values or action values. Consequently, this underscores the necessity to develop new at-

^{*}These authors contributed equally.

[†]Corresponding Author

Copyright © 2024, Association for the Advancement of Artificial Intelligence (www.aaai.org). All rights reserved.

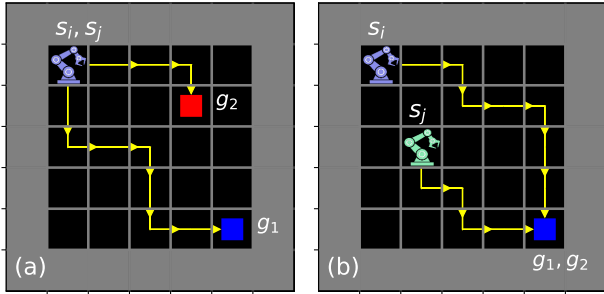


Figure 1: Consider two input tuples (s_i, g_1) and (s_j, g_2) in GCRL. In (a), both tuples share the same state, but g_2 is closer to s_j than g_1 is to s_i . In (b), both tuples share the same goal, but s_i is closer to g_1 than s_j is to g_2 .

tack methods tailored for GCRL to evaluate its robustness. Inspired by adversarial contrastive learning (Kim, Tack, and Hwang 2020; Jiang et al. 2020; Ho and Nvasconcelos 2020), we propose the Semi-Contrastive Representation (SCR) attack, which aims to maximize the distance between representations of original states and their perturbed counterparts, and sidestep the reliance on pseudo labels. Notably, this method can operate independently of the critic function and is readily deployable.

Furthermore, considering the implementation of robust representation training in RL, the bisimulation metric determines two states as equivalent if they share identical rewards and probabilistic transition functions. This method might not be suitable for GCRL. As shown in Fig. 1 (a), even though s_i is closer to its goal g_1 than s_j is to g_2 , both would receive a reward of 0 for not achieving their respective goals. This results in the bisimulation-based distance between $\langle s_i, g_1 \rangle$ and $\langle s_j, g_2 \rangle$ failing to capture their actual proximity. A similar scenario is observed in Fig. 1(b), where the two tuples have identical goals rather than states. Consequently, representation training approaches based on the bisimulation metric encounter hurdles to capture the difference between state-goal tuples in GCRL. As a result, we propose a universal defensive framework named Adversarial Representation Tactics (ARTs). Firstly, we enhance the robustness of vanilla GCRL algorithms with Semi-Contrastive Adversarial Augmentation (SCAA). Secondly, we mitigate the performance degradation associated with bisimulation metric-based robust representation techniques using the Sensitivity-Aware Regularizer (SAR). In summary, our contributions are summarized as follows:

- We introduce the Semi-Contrastive Representation (SCR) attack. It naturally operates without the critic function and is ready for direct deployment.
- We propose a mixed defensive strategy, termed Adversarial Representation Tactics (ARTs), to dynamically enhance adversarial robustness tailored to specific GCRL algorithms.
- Extensive experiments validate that our proposed attack method and defence techniques outperform state-of-the-art algorithms in GCRL by a large margin.

Related Work

Goal-Conditioned Reinforcement Learning

Several methods have tackled GCRL. Hindsight experience replay (Andrychowicz et al. 2018) is often employed to enhance the effectiveness of policies by relabeling the goal. Goal-conditioned supervised learning approaches (Ghosh et al. 2020; Yang et al. 2022) solve this problem by iteratively relabeling and imitating self-generated experiences. For long-horizon tasks, hierarchical RL (Chane-Sane, Schmid, and Laptev 2021) learns high-level policies to recursively estimate a sequence of intermediate subgoals. Moreover, model-based methods (Charlesworth and Montana 2020; Yang et al. 2021a), self-supervised learning (Mezghani et al. 2022; Eysenbach et al. 2022), and planning-based methods (Eysenbach, Salakhutdinov, and Levine 2019; Nasiriany et al. 2019) are also used to solve GCRL problems. Unlike these prior methods, our paper considers the representation training and robustness performance on GCRL.

Adversarial Contrastive Attack

Adversarial contrastive attacks have gained significant attention in recent studies. Particularly, (Kim, Tack, and Hwang 2020) proposes the instance-wise adversarial attack for unlabeled data, which makes the model confuse the instance-level identities of the perturbed data samples. (Jiang et al. 2020) directly exploits the Normalized Temperature-scaled Cross Entropy (NT-Xent) loss to generate PGD attacks. (Ho and Nvasconcelos 2020) introduces a new family of adversarial examples by backpropagating the gradients of the contrastive loss to the network input. While the above methodologies employ varied methods to generate adversaries, they consistently rely on the cosine similarity among the original sample, positive, and negative samples. In this paper, however, we devise a novel contrastive attack method, which is more suitable in GCRL and can be extended to other RL settings.

Bisimulation Metric

Bisimulation metrics offer a framework to gauge the similarity between states within MDPs. The traditional bisimulation metric, as defined by (Ferns, Panangaden, and Precup 2012), considers two states to be close if their immediate rewards and transition dynamics are similar (Larsen and Skou 1989; Givan, Dean, and Greig 2003). This self-referential concept has been mathematically formalized using the Kantorovich distance, leading to a unique fixed-point definition. However, the conventional approach has been criticized for resulting in *pessimistic* outcomes, as it requires consideration of all actions, including those that may be suboptimal. To address this challenge, (Castro et al. 2022) introduced the strategy of Matching Under Independent Couplings (MICo). This approach focuses solely on actions induced by a specific policy π , offering a more optimistic and tailored measure of state equivalence. Whereas, in this work, we focus on their extended version, Simple State Representation (SimSR).

Background

In this section, we first present the fundamental concepts of goal-conditioned MDPs and delve into their extensions in adversarial state-goal scenarios. Then, we outline the architecture of our training backbone and describe SimSR, the cutting-edge robust representation training method.

Goal-Conditioned MDPs

In this section, we model our task as a goal-conditioned MDP. This can be formalized as a tuple $(\mathcal{S}, \mathcal{G}, \mathcal{Z}, \mathcal{A}, r, \gamma, \mathcal{T})$. Here, \mathcal{S} represents the state space, \mathcal{G} the goal space, \mathcal{Z} the latent representation space, and \mathcal{A} the action space. The reward function is denoted by r , γ stands for the discount factor, and \mathcal{T} signifies the state-goal transition probability function.

We assume that the policy function π can be approximated using a combination of an encoder, $\psi(\cdot)$, and an actor network, $\varphi(\cdot)$. The critic function is represented by $\varrho(\cdot)$. Specifically, for any given state $s \in \mathcal{S}$ and goal $g \in \mathcal{G}$, the encoder $\psi(\cdot)$ transforms the concatenated tuple $\langle s, g \rangle$ into the representation space \mathcal{Z} . The resulting feature, $z_{\langle s, g \rangle}$, is expressed as $\psi(\langle s, g \rangle)$. The actor network, $\varphi(\cdot)$, maps this feature, $z_{\langle s, g \rangle}$, to a specific action $a_{\langle s, g \rangle} \in \mathcal{A}$. The action distribution is defined as $a_{\langle s, g \rangle} \sim \pi(\cdot | \langle s, g \rangle)$. Based on the chosen action $a_{\langle s, g \rangle}$, the agent's subsequent state, s' , can be sampled using $s' \sim \mathcal{T}(\cdot | \langle s, g \rangle, a_{\langle s, g \rangle})$ and succinctly represented as $\mathcal{T}_{\langle s, g \rangle}^{\pi}$.

In contrast to traditional RL algorithms, GCRL only provides rewards when the agent successfully achieves a predefined goal. Specifically, we define the reward for a state-goal tuple $\langle s, g \rangle$ as $r_{\langle s, g \rangle} = \mathbb{1}(\mathcal{D}(s, g) \leq \eta)$. Here, η is a predefined threshold, \mathcal{D} acts as a distance metric, determining if s and g are sufficiently close. We utilize ℓ_{∞} -norm in this paper. Given an initial state s_0 and a goal g , our primary objective is to optimize the expected cumulative rewards across joint distributions following:

$$J_{\pi}(s_0, g) = \mathbb{E}_{a_t \sim \pi(\cdot | \langle s_t, g \rangle), \sum_{t=0}^{T-1} \gamma^t r_{\langle s_t, g \rangle}}. \quad (1)$$

In GCRL, the reward function yields only two possible outcomes: 0 or 1, which results in a notably sparser reward sequence $(r_{\langle s_0, g \rangle}, \dots, r_{\langle s_{T-1}, g \rangle})$ over a T -step trajectory compared to other RL algorithms. While these binary rewards may not offer granular insights into the agent-environment interactions, they do guide the agent in a strategy where it initially distances itself from the goal before converging towards it. To derive the optimal policy π^* , we refine Eq. (1) using the Q-value at the initial state s_0 , then $Q_{\pi}(\langle s_0, g \rangle, a_0)$ can be estimated through the Bellman equations:

$$r_{\langle s_0, g \rangle} + \mathbb{E}_{s_1 \sim \mathcal{T}_{\langle s_0, g \rangle}^{\pi}} \max_{a_1 \sim \pi(\cdot | \langle s_1, g \rangle)} Q_{\pi}(\langle s_1, g \rangle, a_1). \quad (2)$$

Definition 1 ((Zhang et al. 2020b)) The adversarial version of a state s can be defined as $\mathcal{V}(s; \theta)$. It is considered stationary, deterministic, and Markovian if its behaviour is solely determined by s and the policy network, which is parameterized by θ . To be simplified, we denote $\mathcal{V}(s; \theta)$ as $\mathcal{V}(s)$.

State-Goal Adversarial Observations

Building on Def. 1, we consider states and goals separately, and individually construct the set of adversarial states $\mathcal{B}_p^{\epsilon}(s)$ and goals $\mathcal{B}_p^{\epsilon}(g)$ using the State-Adversarial MDP (SA-MDP) framework:

$$\begin{aligned} \mathcal{B}_p^{\epsilon}(s) &:= \{\mathcal{V}(s) \mid \|\mathcal{V}(s) - s\|_p \leq \epsilon_s\}, \\ \mathcal{B}_p^{\epsilon}(g) &:= \{\mathcal{V}(g) \mid \|\mathcal{V}(g) - g\|_p \leq \epsilon_g\}, \end{aligned} \quad (3)$$

where ϵ_s and ϵ_g are predefined thresholds of adversarial perturbations on states and goals respectively. $\mathcal{V}(\cdot)$ acts as a stationary and deterministic mapping, which transforms a clean input into its adversarial counterpart. Note that the adversary introduces perturbations solely to the state-goal observations. Consequently, even though the action is determined as $a \sim \pi(\cdot | \langle \mathcal{V}(s), \mathcal{V}(g) \rangle)$, transitions of the environment are still governed by the original state-goal pair $\langle s, g \rangle$, instead of its perturbed counterpart $\langle \mathcal{V}(s), \mathcal{V}(g) \rangle$. Due to uncertainties in the state-goal estimation, there is a potential for generating actions that are not optimal.

Neural Network-based Backbone

In this study, we utilize Multi-Layer Perceptrons (MLPs) of varying depths as the foundational architectures for both the policy function, represented as $\varphi(\psi(\cdot))$, and the critic function, $\varrho(\cdot)$. Specifically, for an encoder $\psi(\cdot)$ comprising L layers, its output, o_L , can be articulated as $o_L = \mathbf{W}_L \phi(\mathbf{W}_{L-1} \cdots \phi(\mathbf{W}_1 o_0))$, with the stipulation that $L \geq 2$. Here, o_0 refers to the input vector in its flattened form, $\phi(\cdot)$ represents the ReLU-based activation function, and \mathbf{W}_i is the weight matrix associated with the i -th layer. To be simplified, we denote the parameters and the depths of $\psi(\cdot)$, $\varphi(\cdot)$, and $\varrho(\cdot)$ as θ_{ψ} , θ_{φ} , θ_{ϱ} , and L_{ψ} , L_{φ} , L_{ϱ} , respectively. For clarity, we choose to omit the bias vector present at each layer.

Simple State Representation (SimSR)

In this paper, SimSR functions as a metric within the representation space, enhancing our base methods in GCRL. Unlike the bisimulation metric (Ferns, Panangaden, and Precup 2012) or MICo (Castro et al. 2022), which employ the Wasserstein or diffuse metric to gauge the distance between two distributions, SimSR adopts a non-diffuse metric, offering a more relaxed approach. Take input tuples $\langle s_i, g_1 \rangle$ and $\langle s_j, g_2 \rangle$ from Fig. 1 for instance, the measurement $\mathcal{M}(\cdot, \cdot)$ between their representations is constructed using the cosine distance (a ℓ_2 normalized dot product distance) as the foundational metric, formulated as:

$$\mathcal{M}(\langle s_i, g_1 \rangle, \langle s_j, g_2 \rangle) = 1 - \frac{\psi(\langle s_i, g_1 \rangle)^{\top} \psi(\langle s_j, g_2 \rangle)}{\|\psi(\langle s_i, g_1 \rangle)\|_2 \|\psi(\langle s_j, g_2 \rangle)\|_2} \quad (4)$$

Note that SimSR shares the same fixed point as MICo. Its update operator can be defined in a manner analogous to MICo.

Theorem 1 ((Zang, Li, and Wang 2022)) Given a policy function π , the SimSR operator T^{π} which defines the state-goal tuple similarity between $\langle s_i, g_1 \rangle$ and $\langle s_j, g_2 \rangle$ can be

updated as:

$$(T^\pi \mathcal{M})(\langle s_i, g_1 \rangle, \langle s_j, g_2 \rangle) = |r_{\langle s_i, g_1 \rangle} - r_{\langle s_j, g_2 \rangle}| + \gamma \mathbb{E}_{s_{i+1} \sim \mathcal{T}_{\langle s_i, g_1 \rangle}^\pi, s_{j+1} \sim \mathcal{T}_{\langle s_j, g_2 \rangle}^\pi} [\mathcal{M}(\langle s_{i+1}, g_1 \rangle, \langle s_{j+1}, g_2 \rangle)], \quad (5)$$

for all $\mathcal{M} : \langle \mathcal{S} \times \mathcal{G} \rangle \times \langle \mathcal{S} \times \mathcal{G} \rangle \rightarrow \mathbb{R}$.

The second term in Eq. (5) is derived through sample-based approximation. Using the SimSR operator, one can iteratively refine the representation by applying it to an arbitrarily initialized $\psi(\cdot)$.

Note that by using cosine distance as the foundational metric in SimSR, all derived state features are normalized to unit length. Furthermore, in contrast to the bisimulation metric which employs the Wasserstein distance, the SimSR operator achieves a computational complexity on par with the MICo operator.

Semi-Contrastive Representation Attack

We present a representation-based adversarial attack for GCRL, which is independent of the critic function and can be seamlessly integrated in the deployment phase.

Limitations of Traditional Attacks in GCRL

Adversarial attacks on states lack the gradient information from labeled examples. To navigate these constraints, existing methods lean on various pseudo-labels, such as Q-values (Zhang et al. 2020b; Kos and Song 2017) or actions (Gleave et al. 2019; Sun et al. 2020) to generate adversarial states. However, as illustrated in Eq. (2), Q-value function is heavily influenced by the reward sequence. Moreover, many of these attacks necessitate access to value networks, making them unsuitable for direct deployment in the inference stage. To address these challenges, we introduce a novel attack method tailored for GCRL algorithms. This approach neither depends on specific pseudo-labels nor requires access to the critic network. Although crafted with GCRL’s unique characteristics, it is versatile enough for broader applications of RL algorithms.

Negative Tuple-Based Adversary

To craft adversaries without relying on labels or pseudo-labels, several studies (Ho and Nvasconcelos 2020; Jiang et al. 2020; Kim, Tack, and Hwang 2020) have introduced the concept of adversarial contrastive attack in the realm of unsupervised learning. Viewed through the lens of representation, an adversary $\mathcal{V}(x)$ for a clean input x is designed to ensure that the feature $f(\mathcal{V}(x))$ diverges significantly from $f(x^+)$ while converging towards the feature of a negative sample, $f(x^-)$. Typically, these methods employ the NT-Xent loss to gauge the similarity among $f(\mathcal{V}(x))$, $f(x^+)$, and $f(x^-)$. This loss can be articulated as:

$$-\log \frac{\sum_{\{x^+\}} \exp(\mathbb{S}(\mathcal{V}(x), x^+))}{\sum_{\{x^+\}} \exp(\mathbb{S}(\mathcal{V}(x), x^+)) + \sum_{\{x^-\}} \exp(\mathbb{S}(\mathcal{V}(x), x^-))}, \quad (6)$$

where $\mathbb{S}(a, b) = \frac{f(a)^\top f(b)}{\tau}$, τ refers to the temperature hyperparameter. Normally, the positive set $\{x^+\}$ can be constructed using different types of data augmentation, such as rotation, color jittering, or scaling, while $\{x^-\}$ indicates

the set of samples collected from other classes. In RL contexts, it is challenging to directly quantify positively correlated samples. Thus, in this section, we present an adversarial contrastive attack approach that exclusively focuses on the negative tuple, termed the Semi-Contrastive Representation (SCR) attack in Def. 2.

Definition 2 (SCR attack) *Given a feature extraction function $f(\cdot)$ and the input tuple $\langle s, g \rangle$, the semi-contrastive representation attack can be defined as follows:*

$$\arg \sup_{\mathcal{V}(s) \in \mathcal{B}_p^c(s), \mathcal{V}(g) \in \mathcal{B}_p^c(g)} \mathbb{E}_{\langle s, g \rangle^-} [\mathcal{L}_{lg}(-f(\langle \mathcal{V}(s), \mathcal{V}(g) \rangle)^\top f(\langle s, g \rangle^-))], \quad (7)$$

where the logistic function $\mathcal{L}_{lg}(v) = \log(1 + \exp(-v))$ for any $v \in \mathbb{R}$, $\langle s, g \rangle^-$ indicates the negative tuple.

It is easy to derive that $\frac{\mathcal{L}_{lg}(v_1) + \mathcal{L}_{lg}(v_2)}{2} \geq \mathcal{L}_{lg}(\frac{v_1 + v_2}{2})$, so we can apply the sub-additivity to the supremum of the values of \mathcal{L}_{lg} by:

$$\begin{aligned} & \sup_{\mathcal{V}(s), \mathcal{V}(g)} \mathbb{E}_{\langle s, g \rangle^-} [\mathcal{L}_{lg}(-f(\langle \mathcal{V}(s), \mathcal{V}(g) \rangle)^\top f(\langle s, g \rangle^-))] \\ & \leq \mathbb{E}_{\langle s, g \rangle^-} \sup_{\mathcal{V}(s), \mathcal{V}(g)} [\mathcal{L}_{lg}(-f(\langle \mathcal{V}(s), \mathcal{V}(g) \rangle)^\top f(\langle s, g \rangle^-))]. \end{aligned} \quad (8)$$

Consequently, we can reframe the challenge of computing the supremum over expectations into determining the expectation over the supremum. This means our goal is to optimize \mathcal{L}_{lg} for a given negative tuple $\langle s, g \rangle^-$. Moreover, leveraging the non-increasing nature of $\mathcal{L}_{lg}(\cdot)$, we can approximate our attack objective by directly minimizing the similarity-based loss $-f(\langle \mathcal{V}(s), \mathcal{V}(g) \rangle)^\top f(\langle s, g \rangle^-)$. In this paper, $f(\cdot)$ is equivalent to $\psi(\cdot)$. Building on this, we present a Projected Gradient Descent (PGD)-based approximation for both $\mathcal{V}(s)$ and $\mathcal{V}(g)$.

Definition 3 (PGD-based Approximation) *Given an encoder $\psi(\cdot)$, an original input tuple $\langle s, g \rangle$, a pre-defined negative tuple $\langle s, g \rangle^-$, and the step size α , then the semi-contrastive representation attack $\mathcal{V}_{scr}(s)$ and $\mathcal{V}_{scr}(g)$ at the iterative step $i + 1$ can be individually defined as:*

$$\mathcal{V}_{scr}^{i+1}(s) = \mathcal{V}_{scr}^i(s) - \alpha \nabla_{\mathcal{V}_{scr}^i(s)} \mathcal{L}_{sim}(s, g, i), \quad (9)$$

$$\mathcal{V}_{scr}^{i+1}(g) = \mathcal{V}_{scr}^i(g) - \alpha \nabla_{\mathcal{V}_{scr}^i(g)} \mathcal{L}_{sim}(s, g, i), \quad (10)$$

Particularly, we define:

$$\mathcal{L}_{sim}(s, g, i) = -\psi(\langle \mathcal{V}_{scr}^i(s), \mathcal{V}_{scr}^i(g) \rangle)^\top \psi(\langle s, g \rangle^-). \quad (11)$$

If the number of iteration steps is $\mathcal{I}(\geq 1)$, then the finally generated adversarial tuple can be defined as $\langle \text{proj}(\mathcal{V}_{scr}^I(s)), \text{proj}(\mathcal{V}_{scr}^I(g)) \rangle$, where $\text{proj}(\cdot)$ is the projection head.

In this work, We denote $\text{proj}(\cdot)$ in Def. 3 as an ϵ -bounded ℓ_∞ -norm ball. In a straightforward yet effective manner, we construct the negative tuple $\langle s, g \rangle^-$ by performing negation operation, including $\langle -s, -g \rangle$, $\langle -s, g \rangle$ and $\langle s, -g \rangle$. By incorporating the SCR attack at each timestep within an episode of T steps in GCRL, our primary aim is to divert the agent, ensuring that it remains distant from the goal. This approach ensures that the reward sequence (r_0, \dots, r_{T-1}) remains as sparse as possible.

To verify the efficacy of our approach, we train multiple agents using diverse GCRL algorithms and evaluate their adversarial robustness against our introduced attack. Comprehensive results are presented in the *Experiments* section.

Adversarial Representation Tactics

As illustrated in Tab. 1 and 2, GCRL agents trained using both base methods and SimSR-strengthened ones are vulnerable to our SCR attack, highlighting a significant security concern. To address this, we introduce a composite defensive strategy termed ARTs in this section, which strategically combine the Semi-Contrastive Adversarial Augmentation (SCAA) and the Sensitivity-Aware Regularizer (SAR), catering to diverse GCRL algorithms.

Semi-Contrastive Adversarial Augmentation

In Algorithm 1, we investigate the influence of data augmentations by subjecting input tuples to the SCR attack. Specifically, during each training epoch for the base GCRL agent, we retrieve a mini-batch of tuples from the replay buffer and generate semi-contrastive augmented samples, $\mathcal{V}_{scr}(s_t^i)$ and $\mathcal{V}_{scr}(g^i)$, using the constructed negative tuples. We then utilize the augmented critic value, denoted as $\hat{\varrho}$, and the actor value, represented as $\hat{\varphi}$, to refine the weights of the encoder (θ_ψ), actor network (θ_φ), and critic network (θ_ϱ). Notably, \mathcal{L}_ψ , \mathcal{L}_φ , and \mathcal{L}_ϱ correspond to the loss functions for the encoder, actor network, and critic network, respectively.

Sensitivity-Aware Regularizer

Given two pairs of observations $(s_i, g_1, r_{\langle s_i, g_1 \rangle}, a_i, s_{i+1})$ and $(s_j, g_2, r_{\langle s_j, g_2 \rangle}, a_j, s_{j+1})$ shown in Fig. 1, it is common that $r_{\langle s_i, g_1 \rangle} = r_{\langle s_j, g_2 \rangle} = 0$, due to the sparsity of reward sequences. Therefore, given the above pair of transitions, we can draw from Thm. 1, and iteratively update the encoder $\psi(\cdot)$ in the policy function using the mean square loss:

$$(\mathcal{M}(\langle s_i, g_1 \rangle, \langle s_j, g_2 \rangle) - \gamma \mathbb{E}_{s_{i+1}, s_{j+1}} [\mathcal{M}(\langle s_{i+1}, g_1 \rangle, \langle s_{j+1}, g_2 \rangle)])^2, \quad (12)$$

where $\mathcal{M}(\langle s_i, g_1 \rangle, \langle s_j, g_2 \rangle)$ is highly dependent on the next states s_{i+1} and s_{j+1} , and rarely captures information from the absolute reward difference $|r_{\langle s_i, g_1 \rangle} - r_{\langle s_j, g_2 \rangle}|$. This cannot provide any evaluations of the difference between state-goal tuples at the current step, and prevents the policy and critic functions from gaining insight from the interaction between the agent and the environment. To compensate for this deficiency of SimSR utilized in GCRL, we construct the Sensitivity-Aware Regularizer as a substitute for $|r_{\langle s_i, g_1 \rangle} - r_{\langle s_j, g_2 \rangle}|$.

Definition 4 (Sensitivity-Aware Regularizer) *Given perturbations $\delta_{s_i}, \delta_{g_1}, \delta_{s_j}, \delta_{g_2}$ for tuples $\langle s_i, g_1 \rangle$ and $\langle s_j, g_2 \rangle$, and a trade-off factor β , the sensitivity-aware regularizer for the encoder $\psi(\cdot)$ can be defined as:*

$$\begin{aligned} & \left| \frac{\mathcal{M}(\langle s_i, g_1 \rangle, \langle s_i + \delta_{s_i}, g_1 \rangle)}{\|\delta_{s_i}\|_2} - \frac{\mathcal{M}(\langle s_j, g_2 \rangle, \langle s_j + \delta_{s_j}, g_2 \rangle)}{\|\delta_{s_j}\|_2} \right| + \\ & \beta \left| \frac{\mathcal{M}(\langle s_i, g_1 \rangle, \langle s_i, g_1 + \delta_{g_1} \rangle)}{\|\delta_{g_1}\|_2} - \frac{\mathcal{M}(\langle s_j, g_2 \rangle, \langle s_j, g_2 + \delta_{g_2} \rangle)}{\|\delta_{g_2}\|_2} \right|, \end{aligned} \quad (13)$$

then we can empirically optimize the encoder parameters θ_ψ using the loss function combining Eq. (12) and Eq. (13).

Algorithm 1: Semi-Contrastive Adversarial Augmentation

Require: Offline dataset \mathcal{D} , learning rate α , training steps T

Initialisation: Critic function $\varrho(\cdot)$, policy function $\varphi(\psi(\cdot))$

```

1: for training timestep  $1 \dots T$  do
2:   Sample a mini-batch from the offline dataset:
       $(s_t^i, a_t^i, s_{t+1}^i, g^i) \sim \mathcal{D}$ 
3:   Construct negative tuples:
       $\langle s_t^i, g^i \rangle^-$  and  $\langle s_{t+1}^i, g^i \rangle^-$ 
4:   Compute the semi-contrastive augmented samples:
       $\mathcal{V}_{scr}(s_t^i)$  and  $\mathcal{V}_{scr}(g^i)$  by Eq. (9-10)
5:   Augment critic value:
       $\hat{\varrho} \leftarrow \mathbb{E}[\varrho(s_t^i, g^i, a_t^i) + \varrho(\mathcal{V}_{scr}(s_t^i), \mathcal{V}_{scr}(g^i), a_t^i)]$ 
6:   Augment actor value:
       $\hat{\varphi} \leftarrow \mathbb{E}[\varphi(\psi(\langle s_t^i, g^i \rangle)) + \varphi(\psi(\langle \mathcal{V}_{scr}(s_t^i), \mathcal{V}_{scr}(g^i) \rangle))]$ 
7:   Update encoder weights:  $\theta_\psi \leftarrow \theta_\psi - \alpha \nabla \mathcal{L}_\psi(\langle s_t^i, g^i \rangle)$ 
8:   Update actor weights:  $\theta_\varphi \leftarrow \theta_\varphi - \alpha \nabla \mathcal{L}_\varphi(\hat{\varphi})$ 
9:   Update critic weights:  $\theta_\varrho \leftarrow \theta_\varrho - \alpha \nabla \mathcal{L}_\varrho(\hat{\varrho})$ 

```

As shown in Def. 4, we explore the Lipschitz constant-based robustness term $\mathcal{M}(\cdot) / \|\delta\|_2$ to indicate the implicit difference. Generally, on the one hand, physically close tuples should have similar Lipschitz constants both on states and goals with a high probability, physically distant tuples. On the other hand, physically distant tuples tend to have dissimilar Lipschitz constants with a high probability. This reflects the similar characteristic as the absolute reward difference utilized in Eq. (5).

Experiments

Our experimental design proceeds as follows: Initially, we identify the optimal representation layer by executing SCR attacks across various layers. Next, we benchmark the SCR attack against other adversarial attacks, using state-of-the-art algorithms as base methods. Finally, we achieve enhanced robustness of different base methods using ARTs.

Baselines

We evaluate our method¹ using four robot manipulation tasks, namely FetchPush, FetchReach, FetchSlide, and FetchPick, as described in (Plappert et al. 2018). The offline dataset for each task is collected through either a purely random policy or a combination of 90% random policies and 10% expert policies, depending on whether the random data sufficiently represents the desired goal distribution. We select 3 algorithms as our baselines for GCRL: Deep Deterministic Policy Gradient (DDPG) (Andrychowicz et al. 2018), Goal-Conditioned Supervised Learning (GCSL) (Ghosh et al. 2020), and Goal-Conditioned F-Advantage Regression (GoFar) (Ma et al. 2022). It is worth noting that to circumvent costly and potentially risky environment interactions, we learn general goal-reaching policies from offline interaction datasets.

¹Our code is available at github.com/TrustAI/ReRoGCRL

Task	Method	Nature	Uniform	SA-FGSM	SA-PGD	Attack Return			SCR-PGD		
						state	SCR-FGSM goal	state+goal	state	goal	state+goal
FetchPick	DDPG	14.82 \pm 1.53	16.68 \pm 4.33	19.61 \pm 2.84	19.92 \pm 2.32	11.18 \pm 2.74	15.00 \pm 1.88	7.83\pm3.06	10.97\pm4.12	16.38 \pm 2.72	10.49\pm2.86
	GCSL	11.39 \pm 1.97	9.95 \pm 1.65	9.94 \pm 1.80	10.07 \pm 1.15	9.52 \pm 2.13	10.41 \pm 1.95	8.99\pm1.56	8.21\pm3.12	11.72 \pm 1.81	8.11\pm2.04
	GoFar	21.01 \pm 2.05	19.91 \pm 2.39	20.07 \pm 2.13	18.92 \pm 1.80	17.14\pm2.89	20.22 \pm 3.25	16.71\pm3.26	17.93 \pm 2.48	19.84 \pm 1.88	15.65\pm1.83
FetchPush	DDPG	12.81 \pm 4.61	13.61 \pm 4.81	17.24 \pm 2.12	15.42 \pm 3.38	8.71\pm3.22	10.27 \pm 3.85	6.43\pm2.33	9.79 \pm 2.15	13.61 \pm 2.56	5.42\pm3.00
	GCSL	12.74 \pm 1.38	12.57 \pm 1.67	9.64 \pm 3.28	9.71 \pm 3.37	9.64 \pm 0.51	12.97 \pm 3.09	8.99\pm1.56	6.20\pm3.66	13.56 \pm 1.49	8.11\pm2.04
	GoFar	18.38 \pm 3.24	16.11 \pm 2.39	15.45 \pm 2.71	13.66 \pm 3.97	11.66\pm3.93	17.47 \pm 2.07	8.19\pm3.99	12.14 \pm 3.78	18.38 \pm 2.91	10.57\pm3.93
FetchReach	DDPG	29.92 \pm 0.20	28.86 \pm 0.46	24.21 \pm 2.21	20.14 \pm 5.04	6.10 \pm 7.33	5.14\pm7.19	2.02\pm3.32	7.02 \pm 2.20	11.03 \pm 8.47	1.86\pm3.31
	GCSL	22.04 \pm 0.68	22.75 \pm 0.82	22.01 \pm 1.47	21.95\pm1.51	20.97\pm1.31	22.24 \pm 0.78	23.04 \pm 1.62	21.74\pm0.81	22.22 \pm 0.79	23.46 \pm 1.14
	GoFar	27.84 \pm 0.63	27.57 \pm 0.92	27.22 \pm 0.49	27.22 \pm 0.49	27.51 \pm 0.45	27.45 \pm 1.11	15.71 \pm 4.48	27.96 \pm 0.38	27.87 \pm 0.33	11.24\pm6.76
FetchSlide	DDPG	0.58 \pm 1.30	1.89 \pm 0.89	0.59 \pm 1.09	0.50 \pm 1.12	0.00\pm0.00	0.36\pm0.72	0.00\pm0.00	0.00\pm0.00	0.38\pm0.60	0.00\pm0.00
	GCSL	1.55 \pm 0.84	1.84 \pm 1.19	0.60 \pm 0.42	0.57 \pm 0.59	0.28\pm0.63	0.97 \pm 0.63	0.37\pm0.51	0.37\pm0.84	0.96 \pm 1.26	0.00\pm0.00
	GoFar	2.55 \pm 1.37	1.23 \pm 1.14	0.77\pm0.92	1.13 \pm 0.72	0.09\pm0.21	1.25 \pm 0.55	0.00\pm0.00	0.00\pm0.00	1.86 \pm 0.73	0.09\pm0.22

Table 1: Comparison of discounted returns for DDPG, GCSL, and GoFar against various attack methods in GCRL. **Red**, **Purple**, and **Blue** individually represent the worst, the second worst, and the third worst returns in each row. The experiments are averaged over 5 seeds.

Task	Nature	Uniform	DDPG (SimSR)			GoFar (SimSR)			SCR-PGD		
			SA-FGSM	SA-PGD	SCR-FGSM	Nature	Uniform	SA-FGSM	SA-PGD	SCR-FGSM	SCR-PGD
FetchPick	16.78	16.00	19.51	17.92	15.74	16.15	17.44	16.73	17.63	13.80	16.27
FetchPush	12.63	15.43	16.24	14.61	10.70	10.51	14.19	13.13	15.52	13.91	12.44
FetchReach	29.90	29.46	28.68	26.76	27.72	27.16	27.93	27.91	27.95	27.96	27.96
FetchSlide	0.62	0.83	0.80	0.43	0.37	0.84	1.66	1.78	2.31	1.41	1.07
											0.59

Table 2: Comparison of discounted returns for DDPG (SimSR) and GoFar (SimSR) against various attack methods in GCRL, averaged over 5 seeds. **Bold** denotes the worst return in each row.

Network Architectures

We use 3-layer MLPs as the backbones of $\varphi(\psi(\cdot))$ and $\varrho(\cdot)$. To determine L_ψ and L_φ , we conduct preliminary experiments based on $\varphi(\psi(\cdot))$, trained via DDPG and GoFar to ascertain the optimal layer for representation. As depicted in Fig. 3, we compute the discounted returns across three distinct layers (Layer 1 denotes the first layer of $\varphi(\psi(\cdot))$, and so forth), with each layer acting as the representation layer. Comprehensive results indicate that Layer 1 is the most susceptible. Therefore, all attacks and training algorithms in this paper are computed on Layer 1.

In particular, the encoder $\psi(\cdot)$ processes the input concatenating a state s and a goal g , which is represented as o_0^π . The dimension of the input tuple is D_{sg} . Thus, we define the latent representation given by $\psi(o_0^\pi) = \phi(\mathbf{W}_1 o_0^\pi)$, $\mathbf{W}_1 \in \mathbb{R}^{256 \times D_{sg}}$. Subsequently, the actor network is constructed as $\varphi(\psi(o_0^\pi)) = \mathbf{W}_4^\pi \phi(\mathbf{W}_3^\pi \phi(\mathbf{W}_2^\pi \psi(o_0^\pi)))$, with $\mathbf{W}_2, \mathbf{W}_3 \in \mathbb{R}^{256 \times 256}$, $\mathbf{W}_4^\pi \in \mathbb{R}^{D_a \times 256}$, where D_a is the dimension of the action. Similar to the policy function π , we construct the output of critic function as $o_4^c = \mathbf{W}_4^c \phi(\mathbf{W}_3^c \phi(\mathbf{W}_2^c \phi(\mathbf{W}_1^c o_0^c)))$, where o_0^c is the concatenation of the tuple $\langle s, g \rangle$ and the action a , which has $(D_{sg} + D_a)$ dimensions. Specifically, $\mathbf{W}_1^c \in \mathbb{R}^{256 \times (D_{sg} + D_a)}$, $\mathbf{W}_2^c, \mathbf{W}_3^c \in \mathbb{R}^{256 \times 256}$, and $\mathbf{W}_4^c \in \mathbb{R}^{1 \times 256}$.

Comparison of SCR and Other Attacks

Following Def. 3, we evaluate the robustness of multiple GCRL algorithms using 5 different attack methods, includ-

ing Uniform, SA-FGSM, SA-PGD, SCR-FGSM, and SCR-PGD. Specifically, we employ a 10-step PGD with a designated step size of 0.01. For both FGSM and PGD attacks, the attack radius is set to 0.1.

Our SCR attack introduces perturbations in the form of $\langle \mathcal{V}(s), g \rangle$, $\langle s, \mathcal{V}(g) \rangle$, and $\langle \mathcal{V}(s), \mathcal{V}(g) \rangle$, respectively. Specifically, Tab. 1-2 and present the results when noise is added solely to the states. We provide the remaining attack results in the Appendix. As outlined in Def. 3, The columns *state*, *goal*, and *state+goal* denote negative tuples as $\langle -s, g \rangle$, $\langle s, -g \rangle$, and $\langle -s, -g \rangle$ individually.

As shown in Table 1, for DDPG-based GCRL, we achieve 47.17%, 57.69%, 93.78%, and 100.00% decrease of discounted returns in FetchPick, FetchPush, FetchReach, and FetchSlide respectively, outperforming SA-based attacks by 60.07%, 64.85%, 90.76%, and 100.00%. In detail, all of them are derived from the negative tuple $\langle -s, -g \rangle$. The results are similar in GCSL, compared with the nature return, our method degrades the performance in FetchPick, FetchPush, and FetchSlide each by 18.41%, 35.68%, and 100.00%. Note that GCSL-based GCRL is more robust in FetchReach than DDPG-based one, our attack can only decrease the performance by 4.46%. As the state-of-the-art algorithm in GCRL, GoFar achieves better nature returns than DDPG and GCSL, thus all attacks exhibit a degradation in their attack capabilities. Particularly, our method achieves a reduction in overall returns of 17.28%, 40.04%, 58.71%, and 100.00% across the four tasks, respectively. Similar to DDPG, the best-performing attack for each of these 4 tasks

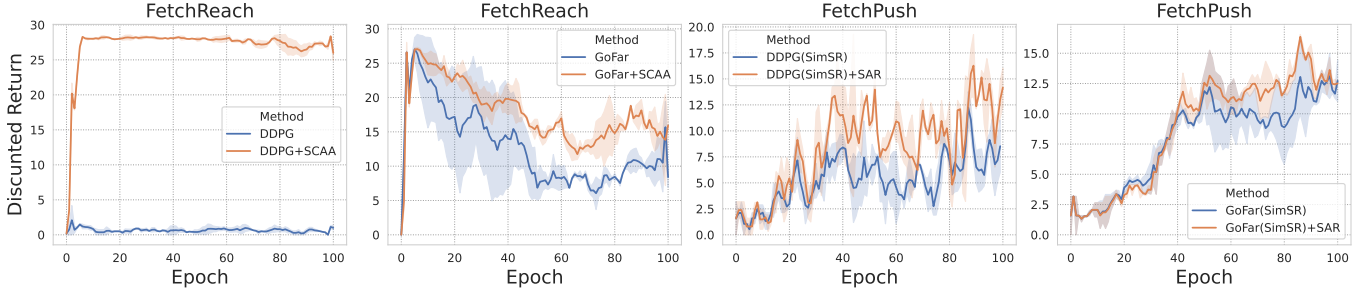


Figure 2: Epoch-wise evaluations on the SCR attack of ARTs-defended DDPG, DDPG (SimSR), GoFar, and GoFar (SimSR).

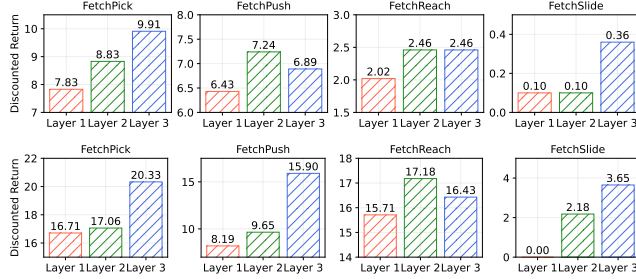


Figure 3: Evaluation of the SCR attack across various layers in MLP-based architectures. The **upper** charts use the DDPG method. The **lower** charts use the GoFar method.

originates from $\langle -s, -g \rangle$.

We further evaluate the adversarial robustness of SimSR-enhanced algorithms as presented in Tab. 2. All attack strategies employ the negative tuple $\langle -s, g \rangle$, notably, our attack surpasses most other attacks when applied to DDPG. In particular, our method outshines the SA attacks by margins of 12.17%, 28.06%, 13.95% in FetchPick, FetchPush, and FetchSlide, respectively. However, when it comes to GoFar, our strategy faces more robust defensive measures. Nevertheless, the SCR attack still achieves a performance boost of 10.57% and 58.16% in FetchPush and FetchSlide compared to SA attacks.

Effectiveness of ARTs

To test the efficacy of ARTs, we correspondingly perform attacks on ARTs-enhanced versions of different GCRL algorithms. Following Alg. 1, we train the agent using the SCR attack. For SimSR-boosted representations, we adaptively employ SAR during the optimization of $\psi(\cdot)$. For simplicity, Tab. 3 only showcases the best attack results from Uniform, SA-FGSM, SA-PGD, SCR-FGSM, and SCR-PGD. All attacks and training procedures in this section are based on $\langle -s, g \rangle$, with perturbations applied solely to the state positions.

As illustrated in Tab. 3, our defensive strategy significantly bolsters the robust performance of DDPG. Specifically, we register performance enhancements of 85.57%, 99.08%, and 1388.17% in FetchPick, FetchPush and FetchReach, respectively. In a similar vein, for DDPG (SimSR), the implementation of ARTs leads to robustness

	Methods	FetchPick	FetchPush	FetchReach	FetchSlide
DDPG	Vanilla	7.83 \pm 3.06	5.42 \pm 3.00	1.86 \pm 3.31	0.00 \pm 0.00
	Vanilla+SCAA	14.53\pm3.08	10.79\pm4.55	27.68\pm1.30	0.00\pm0.00
GoFar	SimSR	15.74 \pm 0.65	10.51 \pm 5.79	27.16 \pm 2.75	0.37 \pm 0.60
	SimSR+SAR	16.78\pm1.39	12.63\pm3.89	29.91\pm0.20	0.55\pm0.20
GoFar	Vanilla	15.65\pm1.83	8.19\pm3.99	11.24 \pm 6.76	0.00 \pm 0.00
	Vanilla+SCAA	14.72 \pm 4.40	8.00 \pm 3.76	13.99\pm6.46	0.00\pm0.00
GoFar	SimSR	13.80 \pm 4.40	12.44\pm3.80	27.91\pm0.34	0.59 \pm 0.66
	SimSR+SAR	14.82\pm3.04	12.44\pm3.80	27.84 \pm 0.32	1.47\pm0.79

Table 3: Defensive performance of ARTs on DDPG, GoFar, DDPG (SimSR), and GoFar (SimSR) against best attacks, averaged over 5 seeds. **Bold** indicates the better result in a block.

improvements of 6.61%, 20.17%, 10.13%, and 48.65% across FetchPick, FetchPush, FetchReach, and FetchSlide, respectively.

For GoFar and its variant, our approach does not appear to achieve the same efficacy as with DDPG and its robust counterparts. However, we still ensure competitive robustness in certain tasks. Specifically for GoFar, our results are comparable and even superior in FetchPush, FetchReach, and FetchSlide. Additionally, for GoFar (SimSR), we observe a performance boost of 7.39% and 149.15%, respectively, in FetchPick and FetchSlide. Complete results are available in the Appendix.

Qualitatively, Fig. 2 provides a visual representation of the epoch-wise performance of ARTs-enhanced GCRL algorithms in comparison to several base methods. In the FetchReach environment, both DDPG+SCAA and GoFar+SCAA exhibit notable improvements within the initial 100 epochs. A similar trend is observed in the FetchPush environment, where SAR boosts the performance of DDPG (SimSR) and GoFar (SimSR) across the majority of epochs.

Conclusion

Due to the sparse rewards in GCRL, we introduce the Semi-Contrastive Representation attack to probe its vulnerability, which only requires access to the policy function. Accordingly, we propose Adversarial Representation Tactics to bolster the robust performance of the underlying agent. Specifically, we devise the Semi-Contrastive Adversarial Augmentation for baseline methods in GCRL and apply the

Sensitivity-Aware Regularizer for their bisimulation metric-guided robust counterparts. Specifically, we employ SimSR to learn invariant representations. Empirical results demonstrate the efficacy of our approaches.

Acknowledgements

This work is supported by the China Scholarship Council (CSC).

References

Andrychowicz, M.; Wolski, F.; Ray, A.; Schneider, J.; Fong, R.; Welinder, P.; McGrew, B.; Tobin, J.; Abbeel, P.; and Zaremba, W. 2018. Hindsight Experience Replay. *arXiv:1707.01495*.

Bai, X.; Guan, J.; and Wang, H. 2019. A model-based reinforcement learning with adversarial training for online recommendation. *Advances in Neural Information Processing Systems*, 32.

Castro, P. S.; Kastner, T.; Panangaden, P.; and Rowland, M. 2022. MICO: Improved representations via sampling-based state similarity for Markov decision processes. *arXiv:2106.08229*.

Chane-Sane, E.; Schmid, C.; and Laptev, I. 2021. Goal-conditioned reinforcement learning with imagined subgoals. In *International Conference on Machine Learning*, 1430–1440. PMLR.

Charlesworth, H.; and Montana, G. 2020. Plangan: Model-based planning with sparse rewards and multiple goals. *Advances in Neural Information Processing Systems*, 33: 8532–8542.

Chebotar, Y.; Hausman, K.; Lu, Y.; Xiao, T.; Kalashnikov, D.; Varley, J.; Irpan, A.; Eysenbach, B.; Julian, R.; Finn, C.; et al. 2021. Actionable models: Unsupervised offline reinforcement learning of robotic skills. *arXiv preprint arXiv:2104.07749*.

Eysenbach, B.; Salakhutdinov, R. R.; and Levine, S. 2019. Search on the replay buffer: Bridging planning and reinforcement learning. *Advances in Neural Information Processing Systems*, 32.

Eysenbach, B.; Zhang, T.; Levine, S.; and Salakhutdinov, R. R. 2022. Contrastive learning as goal-conditioned reinforcement learning. *Advances in Neural Information Processing Systems*, 35: 35603–35620.

Fang, M.; Zhou, C.; Shi, B.; Gong, B.; Xu, J.; and Zhang, T. 2018. DHER: Hindsight experience replay for dynamic goals. In *International Conference on Learning Representations*.

Fang, M.; Zhou, T.; Du, Y.; Han, L.; and Zhang, Z. 2019. Curriculum-guided hindsight experience replay. *Advances in neural information processing systems*, 32.

Ferns, N.; Panangaden, P.; and Precup, D. 2011. Bisimulation metrics for continuous Markov decision processes. *SIAM Journal on Computing*, 40(6): 1662–1714.

Ferns, N.; Panangaden, P.; and Precup, D. 2012. Metrics for Finite Markov Decision Processes. *arXiv:1207.4114*.

Gelada, C.; Kumar, S.; Buckman, J.; Nachum, O.; and Bellemare, M. G. 2019. DeepMDP: Learning Continuous Latent Space Models for Representation Learning. *arXiv:1906.02736*.

Ghosh, D.; Gupta, A.; Reddy, A.; Fu, J.; Devin, C. M.; Eysenbach, B.; and Levine, S. 2020. Learning to Reach Goals via Iterated Supervised Learning. In *International Conference on Learning Representations*.

Givan, R.; Dean, T.; and Greig, M. 2003. Equivalence notions and model minimization in Markov decision processes. *Artificial Intelligence*, 147(1-2): 163–223.

Gleave, A.; Dennis, M.; Wild, C.; Kant, N.; Levine, S.; and Russell, S. 2019. Adversarial policies: Attacking deep reinforcement learning. *arXiv preprint arXiv:1905.10615*.

He, X.; and Lv, C. 2023. Robotic Control in Adversarial and Sparse Reward Environments: A Robust Goal-Conditioned Reinforcement Learning Approach. *IEEE Transactions on Artificial Intelligence*, 1–10.

Ho, C.-H.; and Nivasconcelos, N. 2020. Contrastive learning with adversarial examples. *Advances in Neural Information Processing Systems*, 33: 17081–17093.

Huang, S.; Papernot, N.; Goodfellow, I.; Duan, Y.; and Abbeel, P. 2017. Adversarial attacks on neural network policies. *arXiv preprint arXiv:1702.02284*.

Jiang, Z.; Chen, T.; Chen, T.; and Wang, Z. 2020. Robust pre-training by adversarial contrastive learning. *Advances in neural information processing systems*, 33: 16199–16210.

Kamalaruban, P.; Huang, Y.-T.; Hsieh, Y.-P.; Rolland, P.; Shi, C.; and Cevher, V. 2020. Robust reinforcement learning via adversarial training with langevin dynamics. *Advances in Neural Information Processing Systems*, 33: 8127–8138.

Kim, M.; Tack, J.; and Hwang, S. J. 2020. Adversarial self-supervised contrastive learning. *Advances in Neural Information Processing Systems*, 33: 2983–2994.

Kos, J.; and Song, D. 2017. Delving into adversarial attacks on deep policies. *arXiv preprint arXiv:1705.06452*.

Larsen, K. G.; and Skou, A. 1989. Bisimulation through probabilistic testing (preliminary report). In *Proceedings of the 16th ACM SIGPLAN-SIGACT symposium on Principles of programming languages*, 344–352.

Ma, J. Y.; Yan, J.; Jayaraman, D.; and Bastani, O. 2022. Offline goal-conditioned reinforcement learning via f -advantage regression. *Advances in Neural Information Processing Systems*, 35: 310–323.

Mezghani, L.; Sukhbaatar, S.; Bojanowski, P.; Lazaric, A.; and Alahari, K. 2022. Learning Goal-Conditioned Policies Offline with Self-Supervised Reward Shaping. In *6th Annual Conference on Robot Learning*.

Mezghani, L.; Sukhbaatar, S.; Bojanowski, P.; Lazaric, A.; and Alahari, K. 2023. Learning Goal-Conditioned Policies Offline with Self-Supervised Reward Shaping. In *Conference on Robot Learning*, 1401–1410. PMLR.

Nasiriany, S.; Pong, V.; Lin, S.; and Levine, S. 2019. Planning with goal-conditioned policies. *Advances in Neural Information Processing Systems*, 32.

Pinto, L.; Davidson, J.; Sukthankar, R.; and Gupta, A. 2017. Robust adversarial reinforcement learning. In *International Conference on Machine Learning*, 2817–2826. PMLR.

Plappert, M.; Andrychowicz, M.; Ray, A.; McGrew, B.; Baker, B.; Powell, G.; Schneider, J.; Tobin, J.; Chociej, M.; Welinder, P.; et al. 2018. Multi-goal reinforcement learning: Challenging robotics environments and request for research. *arXiv preprint arXiv:1802.09464*.

Sun, J.; Zhang, T.; Xie, X.; Ma, L.; Zheng, Y.; Chen, K.; and Liu, Y. 2020. Stealthy and efficient adversarial attacks against deep reinforcement learning. In *Proceedings of the AAAI Conference on Artificial Intelligence*, volume 34, 5883–5891.

Weng, T.-W.; Dvijotham, K. D.; Uesato, J.; Xiao, K.; Gowal, S.; Stanforth, R.; and Kohli, P. 2019. Toward evaluating robustness of deep reinforcement learning with continuous control. In *International Conference on Learning Representations*.

Yang, R.; Fang, M.; Han, L.; Du, Y.; Luo, F.; and Li, X. 2021a. MHER: Model-based hindsight experience replay. *arXiv preprint arXiv:2107.00306*.

Yang, R.; Lu, Y.; Li, W.; Sun, H.; Fang, M.; Du, Y.; Li, X.; Han, L.; and Zhang, C. 2021b. Rethinking Goal-Conditioned Supervised Learning and Its Connection to Offline RL. In *International Conference on Learning Representations*.

Yang, R.; Lu, Y.; Li, W.; Sun, H.; Fang, M.; Du, Y.; Li, X.; Han, L.; and Zhang, C. 2022. Rethinking goal-conditioned supervised learning and its connection to offline rl. *arXiv preprint arXiv:2202.04478*.

Zang, H.; Li, X.; and Wang, M. 2022. SimSR: Simple Distance-based State Representation for Deep Reinforcement Learning. *arXiv:2112.15303*.

Zhang, A.; McAllister, R.; Calandra, R.; Gal, Y.; and Levine, S. 2020a. Learning invariant representations for reinforcement learning without reconstruction. *arXiv preprint arXiv:2006.10742*.

Zhang, H.; Chen, H.; Xiao, C.; Li, B.; Liu, M.; Boning, D.; and Hsieh, C.-J. 2020b. Robust deep reinforcement learning against adversarial perturbations on state observations. *Advances in Neural Information Processing Systems*, 33: 21024–21037.

Appendix

In this section, we offer additional experimental details that are not covered in the *Experiments* section of the main manuscript. This encompasses:

- Implementation details for DDPG, GCSL, and GoFar in GCRL.
- Hyperparameters of training algorithms in GCRL.
- Additional SCR attack results for DDPG, GCSL, and GoFar.
- Defensive performance of ARTs on DDPG, GoFar, DDPG (SimSR) and GoFar (SimSR) against SCR-FGSM and SCR-PGD.
- Other definitions for SA and SCR attacks.

Baseline Implementations

DDPG We utilize an open-source implementation of DDPG that has been fine-tuned for the set of Fetch tasks. The objective of the critic network is:

$$\min_Q \mathbb{E}_{(s_t, a_t, s_{t+1}, g) \sim \mathcal{D}} [(r(s_t, g) + \gamma \bar{Q}(s_{t+1}, \pi(s_{t+1}, g), g) - Q(s_t, a_t, g))^2], \quad (14)$$

where \bar{Q} is the targeted Q network. The objective of the policy network is:

$$\min_{\pi} - \mathbb{E}_{(s_t, a_t, s_{t+1}, g) \sim \mathcal{D}} [Q(s_t, \pi(s_t, g), g)]. \quad (15)$$

GCSL GCSL is a straightforward supervised regression method that employs behavior cloning from a hindsight relabelling dataset. We execute the implementation of GCSL by excluding the DDPG critic component and altering the policy loss to adhere to maximum likelihood.

$$\min_{\pi} - \mathbb{E}_{(s_t, a_t, g) \sim \mathcal{D}} [Q(s_t, \pi(s_t, g), g)]. \quad (16)$$

GoFar GoFAR benefits from uninterleaved optimization for its value and policy networks, eliminating the need for hindsight relabeling. They use a discriminator to estimate the reward as below:

$$\mathcal{L}_c(\psi) = \frac{1}{N} \sum_{i=1}^N [\log(1 - c_{\psi}(s_d^j, g^j)) + \frac{1}{M} \sum_{j=1}^M [\log c_{\psi}(s_d^j, g^j)]], \quad (17)$$

The value function is trained as follow:

$$\mathcal{L}_V(\theta) = \frac{1 - \gamma}{M} \sum_{i=1}^M [V_{\theta}(s_0^i, g_0^i)] + \frac{1}{N} \sum_{i=1}^N [f_*(R_t^i + \gamma V(s_{t+1}^i, g_t^i) - V(s_t^i, g_t^i))], \quad (18)$$

Once the optimal V^* has been obtained, the policy is learned via:

$$\mathcal{L}_{\pi}(\phi) = \frac{1}{N} [f'_*(R_t^i + \gamma V_{\theta}(s_{t+1}^i, g_t^i) - V_{\theta}(s_t^i, g_t^i)) \log \pi(a|s, g)], \quad (19)$$

All hyperparameters are kept the same as the original work, and the detailed algorithm can be found in Algorithm 2 in (Ma et al. 2022).

Hyperparameters

In this work, DDPG, GCSL, GoFar share the same network architectures. For all experiments, We train each method for 5 seeds, and each training run uses 100 epochs, containing a minibatch with size 512. The hyperparameters of our backbone architectures and algorithms are reported in Tab. 4.

Task Details

Each of these 4 tasks has continuous state, action, and goal space. The maximum episode horizon is defined as 50. The environments are built upon the 7-degree-of-freedom (DoF) Fetch robotics arm, equipped with a two-fingered parallel gripper. In this section, we provide a detailed introduction to these tasks.

FetchPick In this task, the objective is to grasp an object and transport it to a designated target location, which is randomly selected within the space (e.g., on the table or above it). The goal is represented by three dimensions, specifying the desired object position.

FetchPush In this task, a block is positioned in front of the robot. The robot's actions are limited to pushing or rolling the object to a specified target location. The goal is described by three dimensions, indicating the desired position of the object. The state space encompasses 25 dimensions, encompassing attributes such as the gripper's position, and linear velocities, as well as the position, rotation, and linear and angular velocities of the box.

	Hyperparameter	Value
Training	Optimizer	Adam
	Policy learning rate	1×10^{-3}
	Actor learning rate	1×10^{-3}
	Number of epochs	100
	Number of cycles	20
	Buffer size	2×10^6
	Discount factor	0.98
	Number of Tests	10
	Critic hidden dim	256
	Critic hidden layers	3
	Critic activation function	ReLU
	Actor hidden dim	256
	Actor hidden layers	3

Table 4: Hyperparameters for base methods in GCRL.

Task	Method	Add on s and g						Add on g					
		SCR-FGSM		SCR-PGD		SCR-FGSM		SCR-PGD		SCR-FGSM		SCR-PGD	
		state	goal	state+goal	state	goal	state+goal	state	goal	state+goal	state	goal	state+goal
FetchPick	DDPG	11.18 \pm 2.74	14.79 \pm 1.39	11.39 \pm 3.41	10.84 \pm 3.59	14.97 \pm 1.56	10.16 \pm 2.68	15.70 \pm 3.87	16.94 \pm 2.87	16.76 \pm 2.65	15.11 \pm 2.45	16.38 \pm 2.72	13.31 \pm 2.94
	GCSL	8.06 \pm 2.64	11.14 \pm 1.92	6.10 \pm 2.43	8.18 \pm 3.10	11.30 \pm 1.93	6.12 \pm 3.31	10.85 \pm 1.23	11.66 \pm 1.95	9.73 \pm 2.09	11.17 \pm 2.05	11.72 \pm 1.81	9.48 \pm 2.45
	GoFar	17.14 \pm 2.89	20.98 \pm 2.06	16.23 \pm 2.40	17.83 \pm 2.06	21.01 \pm 2.05	14.77 \pm 2.45	20.63 \pm 2.19	19.78 \pm 1.94	14.79 \pm 3.59	21.03 \pm 2.03	19.84 \pm 1.88	15.40 \pm 2.91
FetchPush	DDPG	6.22 \pm 2.06	11.50 \pm 2.50	4.64 \pm 2.20	9.79 \pm 2.15	12.80 \pm 4.61	6.08 \pm 4.04	12.72 \pm 4.07	12.57 \pm 4.19	13.41 \pm 2.40	11.72 \pm 2.56	13.61 \pm 2.56	8.10 \pm 2.67
	GCSL	5.86 \pm 1.53	12.63 \pm 2.02	5.48 \pm 2.90	6.20 \pm 2.11	12.73 \pm 1.39	6.39 \pm 2.71	12.95 \pm 2.06	13.37 \pm 0.98	11.36 \pm 3.01	12.90 \pm 2.50	13.56 \pm 1.49	10.09 \pm 3.29
	GoFar	11.66 \pm 3.93	18.32 \pm 3.77	10.85 \pm 4.41	14.55 \pm 2.78	18.38 \pm 3.24	11.81 \pm 3.67	16.65 \pm 1.96	16.33 \pm 3.17	10.95 \pm 2.80	18.34 \pm 3.99	18.83 \pm 1.39	10.62 \pm 1.60
FetchReach	DDPG	27.42 \pm 1.32	28.28 \pm 0.70	27.33 \pm 1.43	27.02 \pm 2.20	29.91 \pm 0.20	24.70 \pm 4.07	28.48 \pm 0.55	10.40 \pm 8.64	21.28 \pm 7.45	29.91 \pm 0.20	11.03 \pm 8.47	6.07 \pm 5.32
	GCSL	20.97 \pm 1.31	22.14 \pm 0.76	20.60 \pm 1.26	21.18 \pm 0.95	22.04 \pm 0.68	20.81 \pm 0.95	22.94 \pm 0.75	22.22 \pm 0.79	20.60 \pm 1.26	22.04 \pm 0.68	22.22 \pm 0.79	20.81 \pm 0.95
	GoFar	27.51 \pm 0.45	27.66 \pm 0.95	25.91 \pm 2.02	27.49 \pm 0.94	27.84 \pm 0.63	26.05 \pm 1.85	27.65 \pm 0.80	27.85 \pm 0.34	22.57 \pm 4.15	27.83 \pm 0.65	27.87 \pm 0.33	24.18 \pm 2.43
FetchSlide	DDPG	0.00 \pm 0.00	0.22 \pm 0.32	0.00 \pm 0.00	0.00 \pm 0.00	0.56 \pm 1.27	0.00 \pm 0.00	0.91 \pm 0.95	0.60 \pm 0.55	0.13 \pm 0.31	0.08 \pm 0.18	0.38 \pm 0.60	0.84 \pm 0.68
	GCSL	0.28 \pm 0.63	1.57 \pm 1.06	0.33 \pm 0.74	0.00 \pm 0.00	1.43 \pm 0.62	0.39 \pm 0.89	1.96 \pm 0.98	0.87 \pm 0.52	1.40 \pm 1.38	1.33 \pm 0.67	0.96 \pm 1.26	0.62 \pm 0.80
	GoFar	0.09 \pm 0.21	2.10 \pm 1.38	0.25 \pm 0.55	0.00 \pm 0.00	2.55 \pm 1.37	0.16 \pm 0.22	2.36 \pm 1.46	1.73 \pm 0.74	1.18 \pm 1.17	2.68 \pm 1.01	1.86 \pm 0.73	0.64 \pm 0.73

Table 5: Comparison of discounted returns for DDPG, GCSL, and GoFar against SCR-FGSM and SCR-PGD. The left sub-table shows the attack results added on both s and g , while the right sub-table shows the attack results added on g . The experiments are averaged over 5 random seeds.

FetchReach Within this setting, a 7 DoF robotic arm is tasked with accurately reaching a designated location using its two-fingered gripper. The state space encompasses 10 dimensions, including attributes like the gripper’s position and linear velocities. Correspondingly, the action space is composed of 4 dimensions, representing the gripper’s movements as well as its open/close status.

FetchSlide The FetchSlide environment is similar to FetchPush, involving the control of a 7 DoF robotic arm to slide a box towards a designated location. The key distinction lies in the fact that the target position lies beyond the robot’s immediate reach. Therefore, the robot is required to strike the block in order to initiate its sliding motion towards the target position.

Additional Results of the SCR Attack

Besides the previous attack results shown in Tab. 1 and Tab. 2, we conduct extra experiments in this section. As illustrated in Tab. 5, we evaluate the attack results derived from perturbations on both states and goals and solely on goals.

Full Results for Defensive Performance of ARTs

Building upon the results presented in Tab. 6, we provide a comprehensive analysis of the defensive performance of DDPG, GoFar, and their ARTs-enhanced counterparts. The experimental setup is the same as the *Experiments* section. Details are illustrated in Tab. 6.

FetchPick: Even though all algorithms undergo training with perturbations introduced by the SCR attack, we observed a boost in defensive performance against SA-FGSM for DDPG and DDPG (SimSR). A similar trend is evident against SA-PGD for DDPG (SimSR) and GoFar (SimSR). When defending against SCR-FGSM, the performance improvements are 102.43%, 6.60%, 0.66%, and 7.19% for DDPG, DDPG (SimSR), GoFar, and GoFar (SimSR) respectively. For SCR-PGD, the increments were 38.51%, 3.90%, and 8.26% for DDPG, DDPG (SimSR), and GoFar (SimSR) respectively.

FetchPush: We achieve the performance enhancements when defending against SA-FGSM for DDPG, GoFar, and GoFar (SimSR). Similarly, improvements are observed against SA-PGD for DDPG, GoFar, and GoFar (SimSR). In the context of SCR-FGSM, the increments are 67.81%, 18.04%, 0.85%, and 14.07% for DDPG, DDPG (SimSR), GoFar, and GoFar (SimSR)

Env	ϵ	Method	Nature	Attack Return				
				Uniform	SA-FGSM	SA-PGD	SCR-FGSM	SCR-PGD
FetchPick	0.1	DDPG	14.82 \pm 1.53	16.68 \pm 4.33	19.61 \pm 2.84	19.92 \pm 2.32	7.83 \pm 3.06	10.49 \pm 2.86
		DDPG+SCAA	19.41 \pm 2.59	18.75 \pm 2.65	20.84 \pm 1.47	19.73 \pm 1.93	15.85 \pm 2.65	14.53 \pm 3.08
		DDPG(SimSR)	16.78 \pm 1.39	16.00 \pm 1.68	19.51 \pm 1.05	17.92 \pm 1.65	15.74 \pm 0.65	16.15 \pm 3.49
		DDPG(SimSR)+SAR	16.78 \pm 1.39	18.16 \pm 0.87	19.51 \pm 1.05	18.92 \pm 0.94	16.78 \pm 1.39	16.78 \pm 1.39
		GoFar	21.01 \pm 2.05	19.91 \pm 2.39	20.07 \pm 2.13	18.92 \pm 1.80	16.71 \pm 3.26	15.65 \pm 1.83
		GoFar+SCAA	19.83 \pm 3.94	18.99 \pm 3.57	17.89 \pm 4.13	16.24 \pm 3.86	16.82 \pm 3.46	14.72 \pm 4.40
		GoFar(SimSR)	17.44 \pm 4.40	16.73 \pm 3.81	17.63 \pm 3.61	13.80 \pm 4.40	16.27 \pm 2.75	16.11 \pm 3.49
		GoFar(SimSR)+SAR	17.44 \pm 2.95	17.41 \pm 3.37	17.54 \pm 4.23	14.82 \pm 3.04	17.44 \pm 2.95	17.44 \pm 2.95
FetchPush	0.1	DDPG	12.81 \pm 4.61	13.61 \pm 4.81	17.24 \pm 2.12	15.42 \pm 3.38	6.43 \pm 2.33	5.42 \pm 3.00
		DDPG+SCAA	12.21 \pm 4.16	13.28 \pm 3.72	19.84 \pm 2.50	17.73 \pm 2.77	10.79 \pm 4.55	14.36 \pm 2.90
		DDPG(SimSR)	12.63 \pm 3.89	15.43 \pm 5.36	16.24 \pm 2.42	14.61 \pm 4.41	10.70 \pm 4.55	10.51 \pm 5.79
		DDPG(SimSR)+SAR	10.11 \pm 2.28	13.69 \pm 6.81	16.20 \pm 2.80	14.04 \pm 5.44	12.63 \pm 3.89	12.63 \pm 3.89
		GoFar	18.38 \pm 3.24	16.11 \pm 2.39	15.45 \pm 2.71	13.66 \pm 3.97	8.19 \pm 3.99	10.57 \pm 3.93
		GoFar+SCAA	15.13 \pm 3.23	16.03 \pm 2.44	16.83 \pm 2.59	16.37 \pm 2.87	8.26 \pm 3.66	8.00 \pm 3.76
		GoFar(SimSR)	14.19 \pm 4.49	13.13 \pm 4.68	15.52 \pm 3.88	13.91 \pm 4.49	12.44 \pm 3.80	13.08 \pm 4.08
		GoFar(SimSR)+SAR	14.19 \pm 4.49	12.44 \pm 2.39	16.08 \pm 2.36	14.78 \pm 2.23	14.19 \pm 4.49	14.19 \pm 4.49
FetchReach	0.1	DDPG	29.92 \pm 0.20	28.86 \pm 0.46	24.21 \pm 2.21	20.14 \pm 5.04	2.02 \pm 3.32	1.86 \pm 3.31
		DDPG+SCAA	29.88 \pm 0.14	29.08 \pm 0.31	28.85 \pm 0.39	29.36 \pm 0.21	27.68 \pm 1.30	27.96 \pm 0.91
		DDPG(SimSR)	29.90 \pm 0.18	29.46 \pm 0.40	28.68 \pm 0.97	26.76 \pm 0.98	27.72 \pm 2.35	27.16 \pm 2.75
		DDPG(SimSR)+SAR	29.91 \pm 0.20	29.29 \pm 0.43	28.47 \pm 0.97	27.53 \pm 1.70	29.91 \pm 0.20	29.91 \pm 0.20
		GoFar	27.84 \pm 0.63	27.57 \pm 0.92	27.22 \pm 0.49	27.22 \pm 0.49	15.71 \pm 4.48	11.24 \pm 6.76
		GoFar+SCAA	27.91 \pm 0.36	27.72 \pm 0.27	27.93 \pm 0.35	27.93 \pm 0.35	15.70 \pm 5.03	13.99 \pm 6.46
		GoFar(SimSR)	27.93 \pm 0.34	27.91 \pm 0.34	27.95 \pm 0.33	27.96 \pm 0.32	27.96 \pm 0.29	27.98 \pm 0.33
		GoFar(SimSR)+SAR	27.93 \pm 0.34	27.84 \pm 0.32	27.96 \pm 0.37	27.98 \pm 0.36	27.93 \pm 0.34	27.93 \pm 0.34
FetchSlide	0.1	DDPG	0.58 \pm 1.30	1.89 \pm 0.89	0.59 \pm 1.09	0.50 \pm 1.12	0.00 \pm 0.00	0.00 \pm 0.00
		DDPG+SCAA	0.74 \pm 1.57	1.54 \pm 1.21	1.08 \pm 1.02	0.94 \pm 1.36	0.00 \pm 0.43	0.18 \pm 0.85
		DDPG(SimSR)	0.62 \pm 0.54	0.83 \pm 0.77	0.80 \pm 0.52	0.43 \pm 0.90	0.37 \pm 0.60	0.84 \pm 0.71
		DDPG(SimSR)+SAR	0.62 \pm 0.54	0.61 \pm 0.73	0.55 \pm 0.62	0.63 \pm 1.02	0.62 \pm 0.54	0.62 \pm 0.54
		GoFar	2.55 \pm 1.37	1.23 \pm 1.14	0.77 \pm 0.92	1.13 \pm 0.72	0.00 \pm 0.00	0.00 \pm 0.00
		GoFar+SCAA	1.12 \pm 0.95	1.13 \pm 0.91	0.90 \pm 0.79	0.86 \pm 0.84	0.27 \pm 0.61	0.00 \pm 0.00
		GoFar(SimSR)	1.66 \pm 0.75	1.78 \pm 0.78	2.31 \pm 1.36	1.41 \pm 0.92	1.07 \pm 1.13	0.59 \pm 0.66
		GoFar(SimSR)+SAR	1.66 \pm 0.75	1.95 \pm 1.30	1.47 \pm 0.79	2.25 \pm 1.29	1.66 \pm 0.75	1.66 \pm 0.75

Table 6: Defensive performance of ARTs on DDPG, GoFar, DDPG (SimSR) and GoFar (SimSR) against Uniform, SA-FGSM, SA-PGD, SCR-FGSM, and SCR-PGD attacks. The experiments are averaged over 5 random seeds. **Bold** indicates the best attack result in a row.

respectively. For SCR-PGD, the gains were 164.94%, 20.17%, and 8.49% for DDPG, DDPG (SimSR), and GoFar (SimSR) respectively.

FetchReach: The defence against SA-FGSM sees improvements for DDPG, GoFar, and GoFar (SimSR). Similarly, the performance against SA-PGD also rises for DDPG, GoFar, and GoFar (SimSR). For SCR-FGSM, the gains are 1270.30% and 7.90% for DDPG and DDPG (SimSR), respectively. Against SCR-PGD, the increments are 1403.23%, 10.13%, and 24.47% for DDPG, DDPG (SimSR), and GoFar, respectively.

FetchSlide: Defense improvements against SA-FGSM are observed for DDPG and GoFar, while for SA-PGD, the gains were seen for DDPG, DDPG (SimSR), and GoFar (SimSR). Remarkably, for SCR-FGSM, the improvements were 67.57% and 55.14% for DDPG (SimSR) and GoFar (SimSR) respectively. Against SCR-PGD, the gains were 181.36% for GoFar (SimSR).

Others

To streamline the main text, we reserve some definitions in this section.

Definition 5 (FGSM-based Approximation) *Given an input tuple $\langle s, g \rangle$, attack radius ϵ , and loss function \mathcal{L} , the FGSM-based adversarial state and goal can be individually denoted as:*

$$\begin{aligned} \mathcal{V}(s) &= s + \epsilon \nabla_s \mathcal{L}(\langle s, g \rangle) \\ \mathcal{V}(g) &= g + \epsilon \nabla_g \mathcal{L}(\langle s, g \rangle) \end{aligned} \tag{20}$$

Different from Def. 3, Def. 5 provides a single-step attack on $\langle s, g \rangle$, where $\mathcal{V}(s)$ generated by FGSM is equivalent to $\mathcal{V}^T(s)$ generated by PGD, $\mathcal{V}(g)$ generated by FGSM is equivalent to $\mathcal{V}^T(g)$ generated by PGD. Similar to Def. 3, \mathcal{T} is the number of iteration steps.

Definition 6 (SA attack) *Generally, given an input tuple $\langle s, g \rangle$ and an action a , the SA attack can be defined as follows:*

$$\arg \sup_{\mathcal{V}(s) \in \mathcal{B}_p^\epsilon(s), \mathcal{V}(g) \in \mathcal{B}_p^\epsilon(g)} [-Q(\langle s, g \rangle, a)] \quad (21)$$

Then PGD and FGSM variants of Def. 6 can be analogously represented following Def. 3 and Def. 5.